



Pietro della Casa (Autor)

## Two-step MOVPE, in-situ etching and buried implantation: applications to the realization of GaAs laser diodes

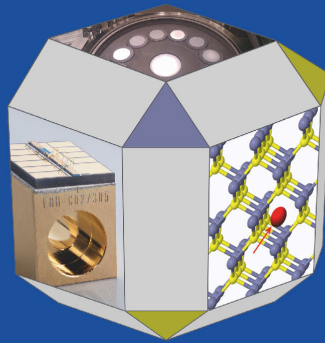


**63**

Forschungsberichte aus dem

Ferdinand-Braun-Institut,  
Leibniz-Institut  
für Höchstfrequenztechnik

Two-step MOVPE, in-situ etching and  
buried implantation: applications to the  
realization of GaAs laser diodes



Pietro della Casa

<https://cuvillier.de/de/shop/publications/8416>

Copyright:

Cuvillier Verlag, Inhaberin Annette Jentzsch-Cuvillier, Nonnenstieg 8, 37075 Göttingen,  
Germany

Telefon: +49 (0)551 54724-0, E-Mail: [info@cuvillier.de](mailto:info@cuvillier.de), Website: <https://cuvillier.de>

# 1 Introduction

This work concerns the use of two-steps epitaxial growth, realized with metalorganic vapor-phase epitaxy (MOVPE), combined with in-situ etching and buried ion implantation, for the realization of GaAs-based edge emitting laser diodes. The fabricated devices fall into two categories: high-power lasers (watt range, multimodal) and tunable lasers (milliwatt range, monomodal).

The experimental work encompasses different investigations, which were in part aimed to get a better understanding of potentials and limitations of the manufacturing technologies - ideally defining some transferrable “building blocks” for device fabrication - and in part more focused on characteristics and performance of the specific devices.

Although a particular emphasis is given to the material-related topics, different aspects – processing, device design and characterization – are often combined in the exposition, as they were in the actual project developments.

The intent of the author is that of presenting the more significant challenges and questions arisen in the various part of the work as “open problems”, and to discuss the possible answers, in the belief that the merit and interest of the exposed material lies essentially in this critical process of understanding.

## Chapters content

**Chapter 2** contains a short, introductory description of III-V Zincblende semiconductors: their main crystalline characteristics, the effect of added or unwanted impurities, their relevance for the realization of optoelectronic devices. A broader – although still very condensed – description of the properties of III-V semiconductors is provided as foundation material appendix 1.

**Chapter 3** presents the MOVPE technology, focusing on the epitaxial reactors and the set of reagents used in this work. A more in-depth discussion of several aspects of the MOVPE process can be found in appendix 2.

In **chapter 4** the in-situ etching with carbon tetrabromide ( $\text{CBr}_4$ ) is studied: the experimental results are presented, including kinetic data, the effects of different etching conditions and of the substrate characteristics. Simple models are proposed to interpret the etching mechanism. Moreover, the possible usefulness of the in-situ etching is discussed, in particular in relation to the problems of reducing surface contamination and enabling in-situ pattern transfer. The in-situ etching has been used in the investigations presented in the following three chapters.

**Chapter 5** deals with the realization of widely-tunable sampled-grating distributed Bragg reflector lasers (SG-DBR). After a general description of the working principle of these devices, the technological aspects of their realization – in particular in relation to the 2-step epitaxy - are presented. Two approaches to the tuning are compared, thermal and electronic. Only the first has led to the realization of working devices, and the reasons behind the difficulties encountered with the second approach are discussed. Fig. 1.1 represents schematically the different sections of the realized SG-DBRs.

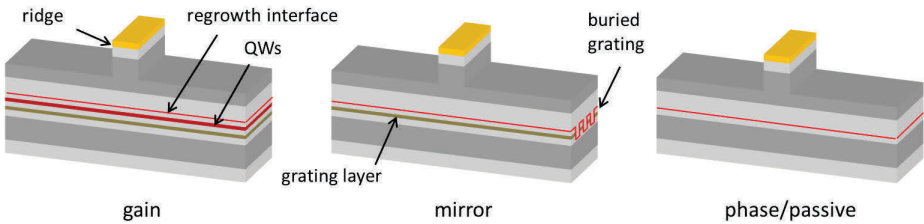


Figure 1.1 Schematic of the different sections of SG-DBR lasers of chapter 5.

**Chapter 6** describes the realization of high-power broad-area lasers (BAL), using a two-step epitaxy process to create a buried, shallow “mesa”, containing the active zone; the approach allows introducing lateral electrical and optical confinement, and simultaneously non-absorbing mirrors (NAM) at the laser facets (Fig. 1.2). Device results are presented and process limitations are discussed.

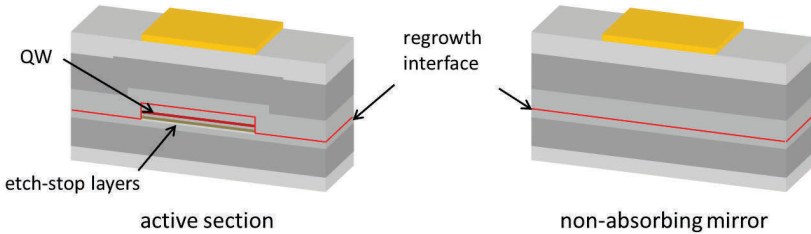


Figure 1.2 Active and passive (NAM) sections of the buried-mesa BALs of chapter 6.

**Chapter 7** presents a different strategy to create deep lateral current confinement in BALs, based on ion implantation *followed* by epitaxial regrowth. Two approaches are compared, one more conservative, where the implantation is done in the upper cladding and the regrowth interface is in a “safe” position (it cannot cause non-radiative recombination) and one more challenging, with the implantation and the regrowth interface both in the waveguide layers (Fig. 1.3). While the first approach has given positive results in term of device performance, the second has proved more problematic; results and possible lessons learned are discussed.

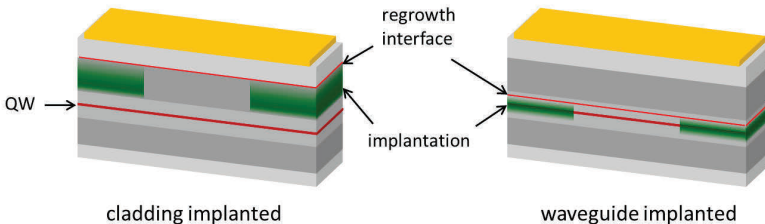


Figure 1.3 Two different positions of implantation and regrowth interface in BALs of chapter 7.

## 2 Zincblende III-V semiconductors

### 2.1 Chapter introduction

This chapter briefly introduces III-V semiconductors, with focus on those that have the same crystal structure of GaAs (Zincblende); only a very few aspects are rapidly touched, selected in an effort to provide a minimal material-related background relevant to the experimental part, without encumbering the narrative with an excessive amount of literature-based information.

Nonetheless, a quite broader – although still extremely condensed - discussion of III-V semiconductors' structural, electrical and optical properties, especially those that are more relevant to the realization of optoelectronic devices, is presented as "foundation material" - and possibly useful reference - in Appendix 1.

### 2.2 Zincblende crystal structure

III-V compounds having As, P and Sb as group V elements crystallize preferably in the Zincblende structure [1].

Within the crystal, each atom has four nearest neighbors of the other species, arranged in a tetrahedron, and the bonding can be interpreted in terms of valence bond theory assuming  $sp^3$  hybridization of both species with formation of four localized sigma bonds, having an ideal angle of  $109.47^\circ$  between each pair.

In Zincblende there are 3 lowest-index high-symmetry families of planes: {100}, {110} and {111}. Figure 2.1 shows a schematic of the corresponding crystal facets and views of atoms and bonds in the crystal, each taken from a direction normal to one of the facets.

The significance of these planes is not only related to symmetry properties but even to chemical reactivity and thermodynamic stability.

Impurity incorporation probability – during the epitaxial growth - can be different between different surfaces. Also the different bonding on different adjacent surfaces can result in different surface diffusion of the atomic species; this is the case for Al and Ga during the growth of the ternary AlGaAs over a patterned surface, resulting in compositional modulation, with zones having a higher or lower Al content. This is generally an unwanted effect in many practical applications, as for example when a ternary or quaternary compound is used for the regrowth over the mesa structure of buried-mesa laser devices, or over the etched Bragg grating in distributed feedback lasers (DFB) and distributed Bragg reflector lasers (DBR), because the compositional perturbation is difficult to control and can even facilitate the formation of extended defects at the conjunction of two growth fronts.

Under surface-reaction-limited conditions, growth and etch rates exhibit selectivity with respect to crystal facets. In the case of growth, the slowest-growing facets emerge over convex substrate geometries, and the fastest-growing facets in the concave; in the case of etch, the situation is reversed, the slowest-etching facets are revealed in concave geometries, the fastest-etching facets over convex geometries. The kinetically more inert faces (slow growth or slow etch) are typically parallel to (111) planes.

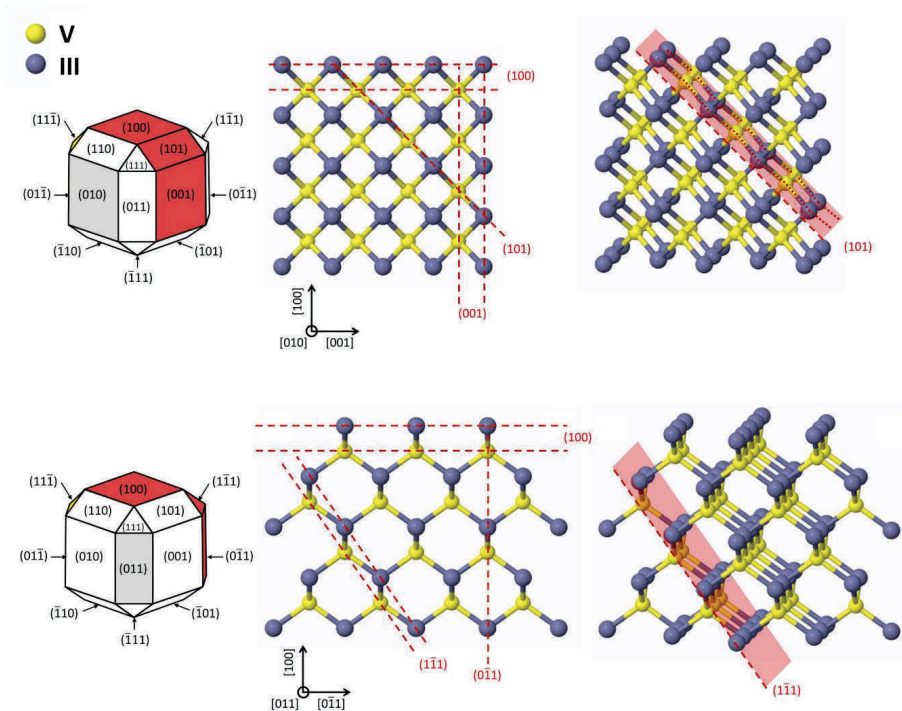


Figure 2.1 Zincblende lowest-index facets and corresponding views of the crystal. The facets in grey are normal to the observation direction, those in red are parallel. The dashed red lines indicate crystal planes perpendicular to the direction of observation. Rightmost, a small twist has been added with respect to the normal view.

The Zincblende Bravais lattice belongs to space group  $F\bar{4}3m$  in Hermann-Mauguin notation ( $T_d^2$  Schoenflies); it is symmorphic<sup>1</sup> and contains 24 point symmetry operations [2]. It does not include an inversion center, a characteristic that allows the onset of an electric field in consequence of the application of strain, because this can shift anions and cations in opposite directions (piezoelectricity). Although Zincblende contains directions, as the  $\langle 111 \rangle$  and  $\langle 100 \rangle$  along which anions and cations are alternated, the unstrained bulk Zincblende crystal has no net polarization because of its overall symmetry.

The  $\{100\}$  planes are perpendicular to the three 4-fold rotoreflection axes and three 2-fold rotation axis of the space group. Along a  $[100]$  direction, there is an alternation of group III and of group V layers: cleavage of the crystal parallel to one  $(100)$  plane leaves a facet terminated either with group III or group V atoms, in both cases with 2 dangling bonds for each atom. Addition or removal of a single atom

<sup>1</sup> A space group is symmorphic when there is a point such that all symmetry operations are the product of a symmetry operation which keeps this point fixed and a translation.

to/from a (100) surface involves no change in the number of dangling bonds. Most commonly, the semiconductor wafers used for device fabrication have a (100) upper surface.

The {110} planes are parallel to the six reflection planes of the space group, the ideal dihedral angle with {100} planes are 45° and 90°. Cleavage parallel to a (110) plane leaves on the surface group III and group V atoms in equal number, with one dangling bond for each atom; within the plane, the atoms are arranged in zigzag chains of consecutively bonded atoms. The cleavage along a (110) plane is facilitated by the absence of polarity in the [110] direction, a characteristic useful for the separation of discrete devices fabricated on (100) oriented wafers, especially when the facets must have optical quality as in the case of edge emitting lasers. Another characteristic, interesting in relation to edge emitter lasers reliability, is that – at least in the case of GaAs - no midgap surface states are expected to be present in ideally cleaved, relaxed (110) surfaces in absence of any oxidation or contamination [3].

The {111} planes are perpendicular to the four 3-fold rotation axes of the space group, the ideal dihedral angle between {111} and {100} planes is 54.74°,  $\frac{1}{2}$  of the tetrahedral bond angle. The {111} planes can be seen as arranged in double layers, each consisting of two closely spaced planes, one containing only group III and the other only group V atoms, with each atom of one layer bonded to 3 of the other layer. These planes are designated with the letters A and B or with the atomic symbols, for example in the case of GaAs  $\{111\}_A \equiv \{111\}_{Ga}$  and  $\{111\}_B \equiv \{111\}_{As}$ . A cleavage parallel to {111} between the A and B planes of a closely-spaced double layer would leave on the surfaces 3 dangling bonds for each atom, while a cleavage parallel to {111} between A and B planes belonging to consecutive double layers would leave only a single dangling bond for each atom.

When the *facet* of a crystal corresponds to a (111) plane, it is designated A or B according to which kind of atom layer *can* terminate the crystal with only *one* dangling bond per atom, assuming the more energetically stable termination: note that in this case, if each atom retains its own electrons, the group V atoms on a type-B facet will have two electrons per dangling bond while the group III atoms on a type-A facet will have no electrons in the dangling bonds<sup>2</sup>. The  $\{111\}_A$  facets are usually the most kinetically stable with respect to chemical etching. The different facets are depicted in Fig. 2.2 along with a representation of a (100) wafer with orientation flats, according to the European-Japanese (E-J) convention.

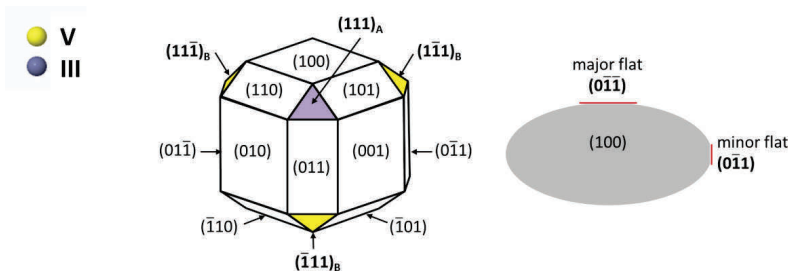


Figure 2.2 Left:  $\{111\}_A$  and  $\{111\}_B$  facets of Zincblende crystal; right: wafer surface and flat orientation, according to E-J convention.

<sup>2</sup> This is not entirely accurate, because the dangling bonds of a non-reconstructed, neutral (111) surface are expected to bear a fractional charge (Appendix 1).

### 2.3 Point defects in III-V semiconductors

Defects related to the presence of foreign atoms are referred to as extrinsic defects. Defects that represent deviations from the regular arrangement of the lattice but are not associated to foreign atoms are called intrinsic.

Among the possible criteria for defects classification, one is based on dimensionality, and divides them into zero-dimensional - or point - defects and extended (1- 2- 3- dimensional). The presence of extended defects is in general unwanted in practical applications; their description goes beyond the scope of this chapter, but basic information has been included in Appendix 1. Point defects [4, 5] are not necessarily detrimental: they contribute in a fundamental way in determining the electrical and optical functionality of semiconductor materials and, moreover, they play a key role in diffusion processes and in device degradation processes.

In semiconductors, the electrons primarily involved in the optical and electrical processes relevant to optoelectronic devices, are those belonging to two separate sets of energetically finely-spaced levels, the valence band (VB) and the conduction band (CB); the difference between the lowest energy level of the CB and the highest energy level of the VB is called bandgap. Electrons in the CB are responsible for n-type conductivity (n-carriers), while empty electronic states (or holes) in the VB are responsible for p-type conductivity (p-carriers).

Electrically active defects introduce one or more energy levels within the bandgap, whose associated electronic wavefunctions are localized. Electrons can be exchanged between these localized levels and the bands.

*Shallow* electronic levels are those whose energy lies near the bottom of the CB or the top of the VB; usually this is intended in the sense that the difference between the level and the nearest band edge is less than the thermal energy  $k_B T$  (26 meV at 300 K). Occupied levels lying near the CB can be easily ionized, promoting electrons into the CB and are called donors; similarly unoccupied levels near the VB can easily accept electrons from the VB, leaving behind a hole, and are called acceptors. The (small) ionization energy of the donors and acceptor makes the electrical conduction an activated process.

*Deep* electronic levels have energies more near the center of the bandgap, with a stronger localization of the electrons (down to the size of an interatomic bond length). The corresponding defects are called deep defects. Some of them are effective electron-traps and/or hole-traps, in the sense that they can capture electrons from the CB or donate electrons to the VB, with the following effects: reduction of carrier density, reduction of carrier mobility via ionized defect formation and increase of non-radiative carrier recombination.

Foreign atoms creating donor or acceptor levels are called dopants; the range of *intentional* doping concentration spans several orders of magnitude, approximately from 0.1 to 1000 ppm. Dopant atoms for III-V semiconductors come usually from the neighboring groups II, IV and VI. They are incorporated in the crystal in the sites normally occupied by a group III or a group V atom, so that the number of the valence electrons of the impurity is higher or lower than that normally contributed by a constituent atom in that lattice position: p doping is obtained decreasing the number of electrons with II $\rightarrow$ III or IV $\rightarrow$ V substitutions, n doping increasing it with IV $\rightarrow$ III or VI $\rightarrow$ V substitutions. Concerning the specific selection of dopants species:

- VI $\rightarrow$ V substitution: S, Se and Te all introduce shallow donor levels; O introduces deep levels and cannot be used as a dopant.
- II $\rightarrow$ III substitutions: Be, Mg (group IIA) Zn and Cd (group IIB), introduce shallow acceptor levels; the other group II elements have not been used successfully for p-doping.
- IV $\rightarrow$ III and IV $\rightarrow$ V substitutions: group IV elements are electrically amphoteric, since they can be simultaneously incorporated in both III and V sublattices, leading to opposite kind of doping. The actual behavior depends on the specific material and from the doping process conditions. In GaAs, C is prevalently incorporated in the group V sites and is a shallow acceptor, Si is incorporated

prevalently in the group III sites where behaves as a shallow donor, Ge is strongly amphoteric, Sn is prevalently a shallow donor.

Silicon, carbon and zinc have been used as dopants in the experimental part of this work, while oxygen has been used to deliberately introduce deep levels.

## 2.4 III-V semiconductors and optoelectronics

III-V semiconductors as GaAs and InP are used in high-speed electronics applications, where their characteristics – in particular higher electron mobility and peak saturation velocity - make them superior to the otherwise more utilized silicon. In the framework of *optoelectronics*, there are two fundamental reasons for their success: first, many of them are efficient light emitters, and second, it is technologically possible to monolithically integrate different material compositions having distinct electrical and optical properties.

The electrons can be excited, in particular by means of current injection or photon absorption, from the – largely occupied – valence band to the – largely empty – conduction band; the reverse disexcitation process can occur through different mechanisms, radiative (photon emission) or non-radiative. Efficient photon emitters are those semiconductors where the photon emission corresponding to the electronic transition from the lowest-energy states of the CB to the highest-energy states of the VB is possible without requiring a change in the momentum (or more properly in the *crystal* momentum) of the electrons. These transitions are called direct, and the semiconductors whose electronic band structure allows such transitions – as is the case for GaAs, InP and many other III-Vs, but not for Si - are called direct semiconductors. Under high-excitation conditions, which are relevant for laser devices, the total recombination rate of a bulk semiconductor (not including stimulated photon emission) is often expressed with the approximate “ABC equation”:

$$R_{tot} = An + Bn^2 + Cn^3, \quad E1.1$$

where  $n$  is the CB electron density; the first term represents the non-radiative recombination caused by the presence of deep levels, the second the (spontaneous) radiative recombination and the third the non-radiative recombination related to carrier-carrier scattering processes (Auger). In a direct semiconductor, the  $B$  coefficient is orders of magnitudes larger than in an indirect one. Of the three coefficients in E1.1,  $B$  and  $C$  stem from the fundamental properties of the material, while  $A$  depends on the kind and density of the defects, and is consequently the only one impacted by the material *quality*.

The monolithic integration of different III-V material compositions in a multilayered, epitaxial crystal structure is fundamentally limited by the necessity to guarantee similar average interatomic distances, or equivalently a similar lattice parameter, in order to avoid the formation of extended defects. Since for technological reasons the available bulk-grown substrates correspond to the binary compounds, the constraint is essentially that of combining the different atomic species, each of them characterized by a different size, in such a proportion that the resulting lattice parameter does not differ too much from that of the substrate, leading to “families” of devices indicated for example as “GaAs-based” or “InP-based”. This leaves anyway a considerable room for the engineering of the material properties.

In the epitaxial growth of a multilayer stack, the transition between different materials can be a technologically critical point, because formation of defects or interlayers with undesirable composition might occur.

Once a laser is realized and tested, the task of determining to which extent the quality of the material and interfaces do actually condition its performance and reliability is – in many cases – not trivial; this will be an important topic in the following parts of the thesis.



### 3 MOVPE growth of III-V compounds

#### 3.1 Introductory remarks on the MOVPE technique [6]

Epitaxy is the process of growing a crystalline material layer on a crystalline substrate, with the layer conforming to the lattice structure of the substrate. It is called homoepitaxy when substrate and layer materials are identical<sup>1</sup> and heteroepitaxy otherwise. Epitaxy is called pseudomorphic when any mismatch between the lattice parameters of the layer and of the substrate is elastically accommodated.

Metalorganic vapor phase epitaxy (MOVPE, also known as metalorganic chemical vapor deposition MOCVD) is the most widespread production method for the realization of light-emitting compound semiconductor devices.

In the MOVPE technique the reagents (or “precursors”) are typically volatile metalorganic compounds (MO) and hydrides, which are transported in the deposition chamber highly diluted in a carrier gas, in most cases hydrogen. The chamber pressure can vary approximately in the range 10 to 1000 mbar, with values between 50 and 150 mbar more commonly used; carrier gas and precursors are kept under laminar flow conditions. The substrates are positioned on a rotating graphite susceptor, whose temperature depends on the material to be grown, and is in the range 550°C-850°C for III-V arsenides and phosphides, while higher temperatures are used for nitrides and lower temperatures for antimonides. Group III precursors are always introduced in lower amount than those of group V, and the growth rate is normally controlled by the diffusion of group III precursors from the gas phase to the substrate; the rate can reach typically some  $\mu\text{m}/\text{h}$ .

The technique is extremely flexible in terms of achievable material compositions, and allows good control over layer thickness, typically in the order of 2% for thick layers (i.e. approximately above 50 nm). Abrupt interfaces between layers of different composition can be obtained: with properly optimized switching sequences, the transition regions can be reduced to the monolayer range. This makes possible the realization of well-defined nanometer size structures, as needed in modern quantum-well lasers.

The experiments described in the present work have been conducted using MOVPE reactors produced by Aixtron SE, of a particular type called *planetary*; two different models were used, AIX2400G3 and AIX2800G4 (abbreviated in the following to **G3** and **G4**). Reactors and precursors are briefly described in the next sections. A more general description of MOVPE can be found in appendix 2.

---

<sup>1</sup> Alternatively, depending on the context, the terms homoepitaxy/heteroepitaxy are used to indicate that substrate and grown layer have/don't have the same crystal structure.

## 3.2 Planetary reactors AIX2400G3 and AIX2800G4 [7-12]

### 3.2.1 Reactor chamber

Planetary reactors look very much alike vertical reactors, but are better described - in terms of flow configuration - as radially-isotropic horizontal reactors. A simplified scheme of the growth chamber is shown in Fig. 3.1; in the drawing, the height of the chamber has been stretched vertically for ease of representation, the actual chamber height/susceptor radius values are 2.6/16.5 cm for G3 and 3.35/31.5 for G4.

The susceptor has a comparatively slow rotation speed, normally in the range 5-25 rpm. The carrier gas with diluted reagents enters the chamber horizontally, through a central injector, and spreads radially; hydrides and MO flows are kept separated in the piping and mix only after injection. The vertical flow velocity - away from the central injector and the edges - is zero, while the radial flow velocity decreases with increasing distance  $x$  from the center. Fluid dynamics modeling [7, 8] shows that in this case the flux of group III to the susceptor - and consequently the growth rate - increases rapidly near the edge of the central injector, and then decreases almost linearly along the radius; more precisely, the decreasing trend can be described with an empirical relation of the form:  $G(x) = a - bx + c/x$ . The group III isobar lines shown in Fig. 3.1 correspond to concentration boundary layer profiles (not to the 99% boundary)<sup>2</sup>.

This radial disuniformity is averaged out by an additional rotation of each wafer around its own center - whence the name planetary.

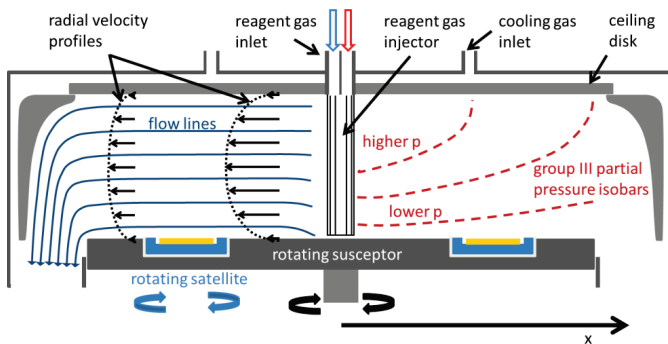


Figure 3.1: simplified scheme of a planetary reactor growth chamber, with qualitative representation of flow lines and group III isobar lines; the height of the chamber has been stretched with respect to real proportion for ease of representation.

The wafers are positioned over small graphite disks, called satellites, which are inserted in recesses within the susceptor. The surface of these recesses is not flat, but contains shallow spiral grooves, each with a small gas outlet, as can be seen in Figure 3.2a which shows the planetary susceptor with satellites removed.

The satellites are free to rotate around a metal pin protruding from the center of the recess, while a gas flow, normally of  $H_2$ , coming from inside the susceptor lifts them (by some tens  $\mu m$ ) eliminating the friction and providing a viscous shear force for their rotation (gas-foil rotation). The gas is then

<sup>2</sup> For a discussion of boundary layer approximation, see appendix 2.